NASA Conference Publication 2404

Numerical Techniques in Acoustics

Extended abstracts of papers to be presented at American Society of Mechanical Engineers Winter Annual Meeting, Miami Beach, Florida, November 17–21, 1985

NASA

NASA Conference Publication 2404

Numerical Techniques in Acoustics

Compiled by
Kenneth J. Baumeister
NASA Lewis Research Center
Cleveland, Ohio

Extended abstracts of papers
to be presented at American
Society of Mechanical Engineers
Winter Annual Meeting, Miami Beach,
Florida, November 17–21, 1985

National Aeronautics
and Space Administration

**Scientific and Technical
Information Branch**

1985

FOREWORD

The Numerical Techniques in Acoustics Forum of the Noise Control and Acoustics Technical Division of the American Society of Mechanical Engineers provides an opportunity for presenting, at the earliest possible time, current work in the various aspects of numerical techniques in acoustics. The informal nature of the forum encourages the presentation of results that are not yet complete enough for formal presentation and the discussion of these results while work is still current. When the results of the investigations presented at this forum are confirmed by analysis or experiment, the ASME encourages the authors to document their research as formal papers for possible publication in the transactions of the society.

As part of this forum, it is intended to allow the participants time to raise questions on unresolved problem areas and to generate discussions on possible approaches and methods of solution.

The papers in this proceedings are arranged according to the planned order of presentation at the 1985 ASME Winter Annual Meeting in Miami Beach, Florida.

Dr. Kenneth J. Baumeister
NASA Lewis Research Center
Cleveland, Ohio 44135

CONTENTS

APPLICATION OF HIGH ORDER ACOUSTIC FINITE ELEMENTS TO TRANSMISSION LOSSES AND ENCLOSURE PROBLEMS

A. Craggs and G. Stevenson
University of Alberta
Edmonton, Alberta, Canada T6G 2G8

A family of acoustic finite elements has been developed based on C° continuity (acoustic pressure being the nodal variable) and the no–flow condition. The family includes triangular, quadrilateral and hexahedral isoparametric elements with linear, quadratic and cubic variation in modelling and distortion. Of greatest use in problems with irregular boundaries are the cubic isoparametric elements: the 32 node hexahedral element for three–dimensional systems; and the twelve node quadrilateral and ten node triangular elements for two–dimensional/axisymmetric applications. These elements have been applied to problems involving cavity resonances, transmission loss in silencers and the study of end effects, using a Floating Point Systems 164 attached array processor accessed through an Amdahl 5860 mainframe.

Accuracy of the cubic elements is quite good, requiring only two elements per standing wavelength in a rectangular room cavity resonance problem to produce eigenvalues with less than 0.5% error.

The elements are presently being used to study the end effects associated with duct terminations within finite enclosures. The model utilized in this study is essentially a helmholtz resonator which consists of two cavities connected by a duct, the overall enclosure being symmetric about the midpoint of the duct. By solving for the lowest non–zero eigenpair, the acoustic pressure contours can be plotted (see figure 1 for example) and the equivalent attached mass calculated. Through variations in the geometry of the duct termination and the location of the cavity walls, design criteria are being developed.

The transmission losses associated with various silencers and sidebranches in ducts is also being studied using the same elements. The inlet and outlet ducts are modelled as having infinite lengths and the inlet and outlet waves are forced to be plane. Both the transmission loss spectrum for a particular frequency range and the pressure profile for a specific frequency can be generated. As a test of both the program and the elements, a comparison was done with experimental data gathered by Blaser and Chung (1) for an expansion chamber silencer. The model of the silencer was based on the use of two quadrilateral cubic elements per wavelength over the frequencies of interest, and the resulting transmission loss spectrum is very close to the experimental (see figure 2).

(1) D.A. Blaser and J.Y. Chung 1978 *Proceedings - International Conference on Noise Control Engineering: Inter-Noise '78.* A transfer function technique for determining the acoustic characteristics of duct systems with flow.

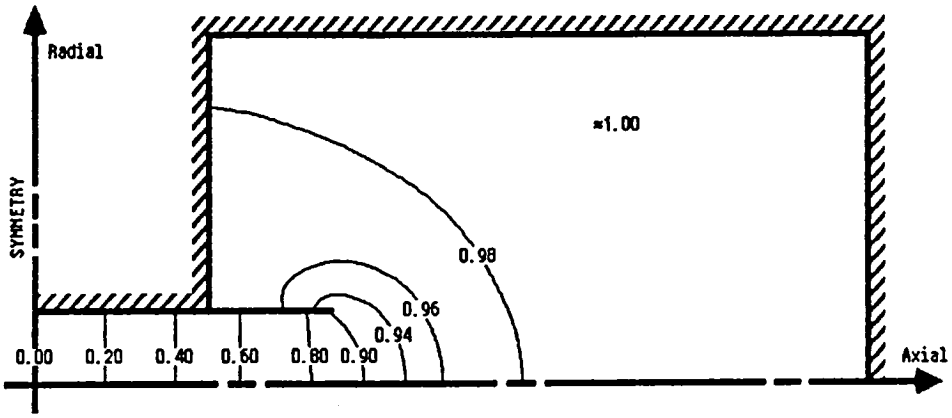

RELATIVE PRESSURE CONTOURS FOR A SHARP–EDGED CIRCULAR DUCT

Figure 1

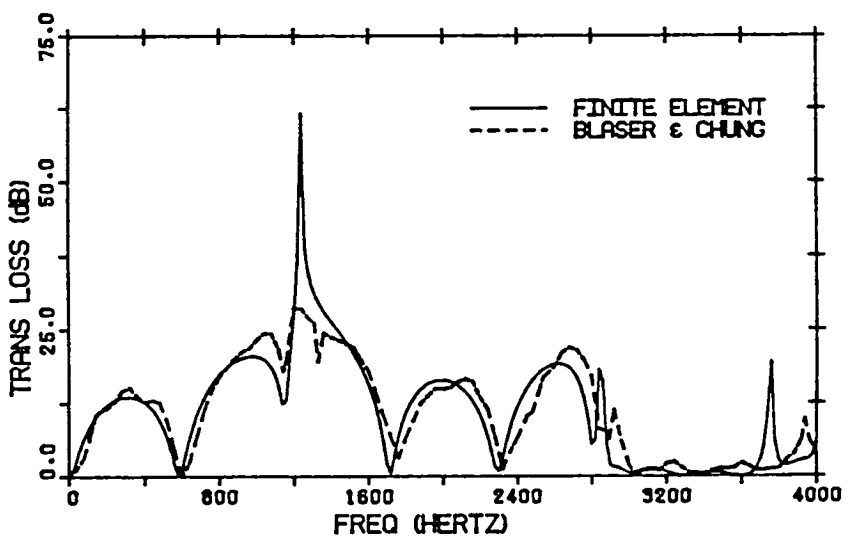

COMPARISON TO EXPERIMENTAL DATA FOR SILENCER

Figure 2

ON THE COMPUTATION OF STRUCTURAL VIBRATIONS INDUCED BY A LOW-SPEED TURBULENT FLOW

Y.F. Hwang
David Taylor Naval Ship R&D Center
Bethesda, Maryland 20084

This paper discusses a method for numerical evaluation of the vibrations of a cylindrical shell structure induced by a low-speed external turbulent flow. The direction of flow is along the axis of revolution of the shell (see Figure 1), and the source of excitation is the pressure fluctuations in the turbulent boundary layer (TBL).

For the investigation of vibration and noise problems it is usually more desirable to utilize the modal expansion approach. The axisymmetric shell structure shown in Figure 1 can be modeled by the assemblage of conical-shell finite-elements. This modeling allows the eigenfunction $\psi_{mn}(x,\theta)$ to be represented in a rectangular product of a longitudinal modal function $f_{mn}(x)$ and a circular harmonic function cos $m\theta$ (or sin $m\theta$), i.e.,

$$\psi_{mn}(x,\theta) = f_{mn}(x) \cos m\theta \qquad (1)$$

$$m=0,\ 1,\ 2,\ \ldots$$

$$n=1,\ 2,\ 3,\ \ldots$$

The forcing function from the TBL is assumed to be spatially homogeneous and temporally stationary. It is commonly expressed in terms of the wavevector-frequency spectrum $\Phi_p(k_1,k_3,\omega)$ where k_1 is the streamwise wavenumber and k_3 is the transverse wavenumber. For the calculation of the structural acceptance with this forcing function, the structural modes must also be expressed in wavenumber space. This can be accomplished by taking a spatial Fourier transform of the modes. The finite-element modeling provides the computed eigenfunction defined at a set of discrete points. If the grid points on the flow surface are equally spaced, a Fast Fourier Transform (FFT) routine may be used. From the FFT spectral coefficients, we may express

$$f_{mn}(x) = a_o + \sum_{\nu=1}^{U} \left[a_\nu \cos \frac{2\nu\pi}{L} x + b_\nu \sin \frac{2\nu\pi}{L} x\right] \qquad (2)$$

where U is one less than one half of the total number of FFT data points and L is the axial length of the structure.

The effective modal input spectral density $\pi_{mn}(\omega)$ from the TBL can be evaluated as follows,

$$\pi_{mn}(\omega) = A^2\ \phi(\omega)\ J^2_{mn,mn}(\omega) \qquad (3)$$

where A is the total area of the flow surface, $J^2_{mn,mn}(\omega)$ is the modal joint-acceptance (or called self-acceptance), which provides a measure of the degree of coupling between the turbulent pressure field and the structure, and $\phi(\omega)$ is the frequency spectrum of the TBL pressure fluctuations. The joint-acceptance can be computed by the following summation, i.e.,

$$J^2_{mn,mn}(\omega) = [(2\pi)^3/A\phi(\omega)]$$

$$\times \left[a_o^2\, \Phi_p(0,\frac{m}{R},\omega) + \frac{1}{2}\sum_{\nu=1}^{U} (a_\nu^2+b_\nu^2)\, \Phi_p(\frac{2\nu\pi}{L}, \frac{m}{R},\omega)\right] \tag{4}$$

where R is the radius of the cylindrical shell.

Often it is required to evaluate the summation up to the convection wavenumber. This requires that the number of FFT data points to be approximately $\omega L/\pi U_c$, where U_c is the convection velocity of the TBL. If the length L of the structure is large and the frequencies of interest are high, the required data points will generally exceed the number of finite-element grid points. This difficulty can be overcome by obtaining additional data points from spline fitting and interpolation of the eigenfunctions.

If the size of structure is larger than the correlation length of the pressure field, the cross-modal acceptance $J^2_{mn,m'n'}(\omega)$, can be neglected. In this case, the structural displacement response spectrum $[s(\omega)]$ evaluated at $\theta = \theta_o$ can be calculated as follows:

$$[s(\omega)] = [\psi][H^*_{mn}(\omega)][\pi_{mn}(\omega)][H_{mn}(\omega)][\psi]^T \tag{5}$$

where $[\psi]$ is the assembly of eigenvectors, each column represents one eigenvector $\{f_{mn}(x_i)\cos m\theta_o\}$. $H_{mn}(\omega)$ is the modal admittance function which is defined as

$$H_{mn}(\omega) = \{M_{mn}[(\omega^2_{mn}-\omega^2) + i(\omega^2_{mn}\,\eta_{mn}+\omega\omega_{mn}\,\delta_{mn})]\}^{-1} \tag{6}$$

and where M_{mn} is the mode mass, η_{mn} is the structural modal loss factor, and δ_{mn} is the modal acoustic loss factor.

The most difficult task in the numerical evaluation of flow induced vibration is the uncertainty about the forcing functions, i.e., the wavevector-frequency spectrum. Several theoretical forcing function models have been published in recent years, all of them require an empirical fit with experimental data. Published experimental data are very widely scattered depending on the measuring facility, surface property, the method of scaling the data, etc. Selection of a suitable forcing function model and the experimental data thus depend heavily on experienced engineering judgement and knowledge of how the experimental data are obtained.

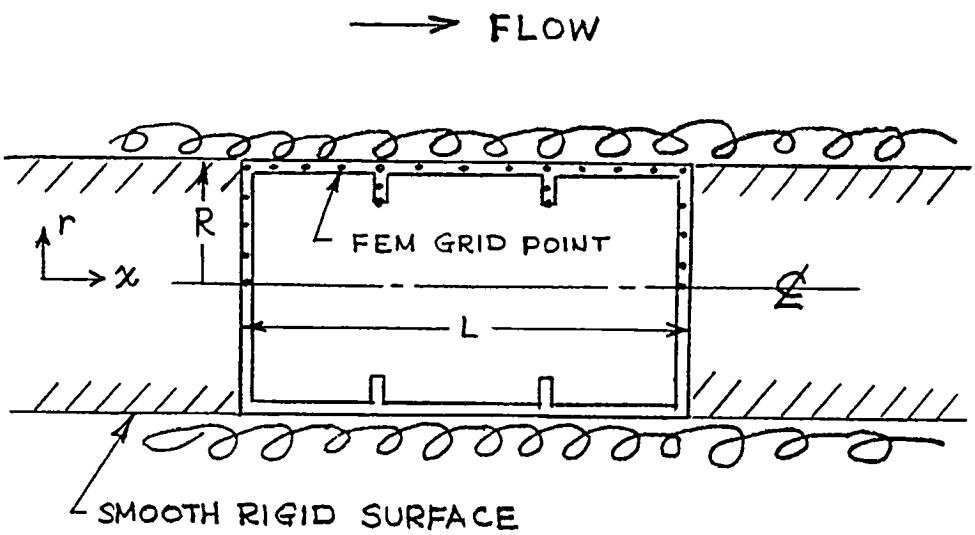

FIG. 1 A CYLINDRICAL SHELL STRUCTURE WITH AN EXTERNAL TURBULENT FLOW

IMPROVING THE ACCURACY OF THE BOUNDARY INTEGRAL METHOD

BASED ON THE HELMHOLTZ INTEGRAL

G.H. Koopmann and K. Brod
University of Houston - University Park
Houston, Texas 77004

Several recent papers in the literature have been based on various forms of the Helmholtz integral to compute the radiation fields of vibraing bodies. The surface integral has the form

$$P(R_0) = \frac{1}{2\pi} \oint_S \left[i\omega\rho G(R,R_0)\, V(R_0) - \frac{\partial G}{\partial n}(R,R_0) P(R_0) \right] dS_0$$

where the symbols P, R_0, w, ρ, G, R, V, and S_0 are acoustic pressure, source coordinate, angular frequency, fluid density, Green function, field coordinate, surface velocity and body surface respectively. A discretized form of the surface integral is

$$\begin{bmatrix} \delta_{ij} - D_{ij} \end{bmatrix} \begin{bmatrix} P_j \end{bmatrix} = \begin{bmatrix} M_{ij} \end{bmatrix} \begin{bmatrix} V_j \end{bmatrix}$$

where D and M are the dipole and monopole coefficients and i and j are the field and source coordinates. Solutions to the above surface integral are complicated with the singularity of the Green function at $R=R_0$ and with the uniqueness problem at interior eigen frequencies of the enclosed space. The use of the interior integral circumvents the the singularity problem since the field points are chosen in the interior space of the vibrating body where a zero pressure condition exists. The interior integral has the form

$$\oint_S \frac{\partial G}{\partial n}(R,R_0) P(R_0)\, dS_0 = \oint_S i\omega\rho G(R,R_0)\, V(R_0) dS_0$$

The discretized version of the integral relates the surface pressure to the surface velocity through a transfer function, T_{ij} as

$$\left[P_j\right] = \left[T_{ij}\right]\left[V_j\right]$$

In the above form, the field points are located in the interior space enclosed by the surface of the body. In general, we have found that T_{ij} is not invariant with choice of interior points, i.e., different sets of interior field points produce different sets of surface pressures. (It can be shown that the same problem exists for the surface integral applications). T_{ij} can be made invariant (or nearly so) by placing a stronger condition on the pressure field in the interior space. With a finite set of of interior points, the requirement that the zero pressure condition exists everywhere in the interior volume is not met. To satisfy this requirement, the interior equation can first be integrated over an incremental interior volume ΔV_k as

$$\int_{\Delta V_k} \left[\oint_S \left\{ \frac{\partial G}{\partial n}(R,R_0) P(R_0) - i\omega\rho G(R,R_0)\, V(R_0) \right\} dS_0 \right] dV$$

which, after the volume integral integration gives

$$\oint_S \left\{ \frac{\partial G_k}{\partial n}(R_0)\, P(R_0) - i\omega\rho G_k(R_0)\, V(R_0) \right\} dS_0$$

Breaking up the interior space into the same number of elemental volumes as surface elememts produces a discretized form of the interior equation as

$$\left[P_j\right] = \left[T_{Kj}\right]\left[V_j\right]$$

An added advantage of satisfying the field pressure condition in the interior volume is that the uniqueness problem associated with the interior eigen modes is eliminated since the interior pressure is necessarily zero at all frequencies. Examples of the above method will be presented for a variety of radiators.

A NUMERICAL METHOD OF CALCULATING PROPELLER NOISE INCLUDING ACOUSTIC NONLINEAR EFFECTS*

K.D. Korkan**
Texas A&M University
College Station, Texas 77843

Using the transonic flow fields(s) generated by the NASPROP-E computer code[1] for an eight blade SR3-series propeller, a theoretical method is investigated to calculate the total noise values and frequency content in the acoustic near and far field without using the Ffowcs Williams - Hawkings equation[2]. The flow field is numerically generated using an implicit three-dimensional Euler equation solver in weak conservation law form. Numerical damping is required by the differencing method for stability in three dimensions, and the influence of the damping on the calculated acoustic values is investigated. Since the propeller flow field includes the wave systems near the propeller blade surface, the quadrupole noise source term is accounted for as are the monopole and dipole noise sources. The acoustic near field is solved by integrating with respect to time the pressure oscillations induced at a stationary observer location. The frequency spectrum at the specified observer location is calculated by representing the pressure time-history by a Fourier series and calculating the noise levels for an appropriate number of harmonics of the fundamental frequency[3,4]. Comparisons between the theoretical model and the experimental results of Dittmar, et.al[5] have been made for the SR-3 propfan, and found to be within 4% for the acoustic near field in the propeller disc plane[6]. The acoustic far field is calculated from the near field primitive variables as generated by NASPROP-E computer code using a method involving a perturbation velocity potential as suggested by Hawkings[7] in the calculation of the acoustic pressure time-history at a specified far field observed location. The methodologies described are valid for calculating total noise levels and are applicable to any propeller geometry for which a flow field solution is available.

References

1. Bober, L.J., Chausee, D.S. and Kutler, P., "Prediction of High Speed Propeller Flow Fields Using a Three-Dimensional Euler Analysis," NASA TM 83065, January 1983.

2. Ffowcs Williams, J.E., and Hawkings, D.L., "Sound Generated by Turbulence and Surfaces in Arbitrary Motion," Philosophical Transactions of the Royal Society of London, Vol. A264, 1969.

*This work is supported by NASA Lewis Research Center Grant NAG 3-354.
**Associate Professor, Aerospace Engineering Department.

3. Korkan, K.D., von Lavante, E. and White, T.A., "An Alternative Method of Calculating Propeller Noise Generated at Transonic Tip Speeds, Including Non-Linear Effects," AIAA Paper 85-0002, January 1985.

4. White, T.A., "Numerical Evaluation of Propeller Noise, Including Non-Linear Effects," Master of Science Thesis, Aerospace Engineering Department, Texas A&M University, May 1985.

5. Dittmar, J.H. and Jeracki, R.J., "Additional Noise Data on the SR-3 Propeller," NASA TM 81736, May 1981.

6. Korkan, K.D., von Lavante, E., and Bober, L.J., "Numerical Evaluation of Propeller Noise Including Non-Linear Effects," AIAA Paper 84-2301, October 1985, (Submitted to AIAA J. for publication).

7. Hawkings, D.L., "Noise Generation by Transonic Open Rotors," Research Paper No. 599, Westland Helicopters Limited, June 1979.

A GENERAL-APPLICATIONS DIRECT GLOBAL MATRIX ALGORITHM FOR RAPID SEISMO-ACOUSTIC WAVEFIELD COMPUTATIONS

Henrik Schmidt
SACLANT R&D Center
La Spezia, Italy

Gerard J. Tango and Michael F. Werby
National Space Technology Laboratories
NSTL Station, Mississippi 39529-5004

The purpose of this paper is to explain and illustrate a new matrix method for rapid wave propagation modeling in generalized stratified media, which has recently been applied to numerical simulations in diverse areas of underwater acoustics, solid earth seismology, and nondestructive ultrasonic scattering.

This report summarizes a portion of recent efforts jointly undertaken at NATO SACLANT and NORDA Numerical Modeling groups in developing, implementing, and testing a new fast general-applications wave propagation algorithm, SAFARI, formulated at SACLANT by Schmidt (1982). Historically, most algorithms for computing acoustic transmission loss, synthetic seismic time series, and ultrasonic beam scattering have been separate applications-specific programs, using a (local) Thomson-Haskell propagator matrix to recursively propagate the complete wavefield solution across all layers. In contrast, the present general-applications SAFARI program uses a Direct Global Matrix Approach to multilayer Green's function calculation. A rapid and unconditionally stable solution is readily obtained via simple Gaussian elimination on the resulting sparsely banded block system, precisely analogous to that arising in the Finite Element Method. The resulting gains in accuracy and computational speed allow consideration of much larger multilayered air/ocean/earth/engineering material media models, for many more source-receiver configurations than previously possible. The general multisource capability allows choice of number and location of point or line sources, for monofrequency transfer function, field contour or beam analysis, and broadband pulse modeling, in plane or cylindrical geometries, for a general n-layered system. The only effective limit is computer virtual memory, which on a VAX 11/780 + FPS 164, allows as many as 250 layers/100 receivers/50 sources/2000 Hz bandwidth.

We demonstrate the validity and versatility of the SAFARI-DGM method by reviewing three practical examples of engineering interest, drawn from ocean acoustics, engineering seismology and ultrasonic scattering. Extension of these results to further infrasonic and atmospheric noise modeling (as well as nondestructive evaluation) is immediate.

References

Pekeris, C. L., 1948. "Theory of Propagation of Explosive Sound in Shallow Water." *Geol. Soc. Am. Memoirs*, no. 27.

Schmidt, H., 1982. "Excitation and Propagation of Marine Seismic Interface Waves (using a new Fast Field Program)," in: N. G. Pace (ed.), *Acoustics and the Seabed*, Institute of Acoustics Proceedings. Bath UK: University Press.

SAFARI NUMERICAL MODEL

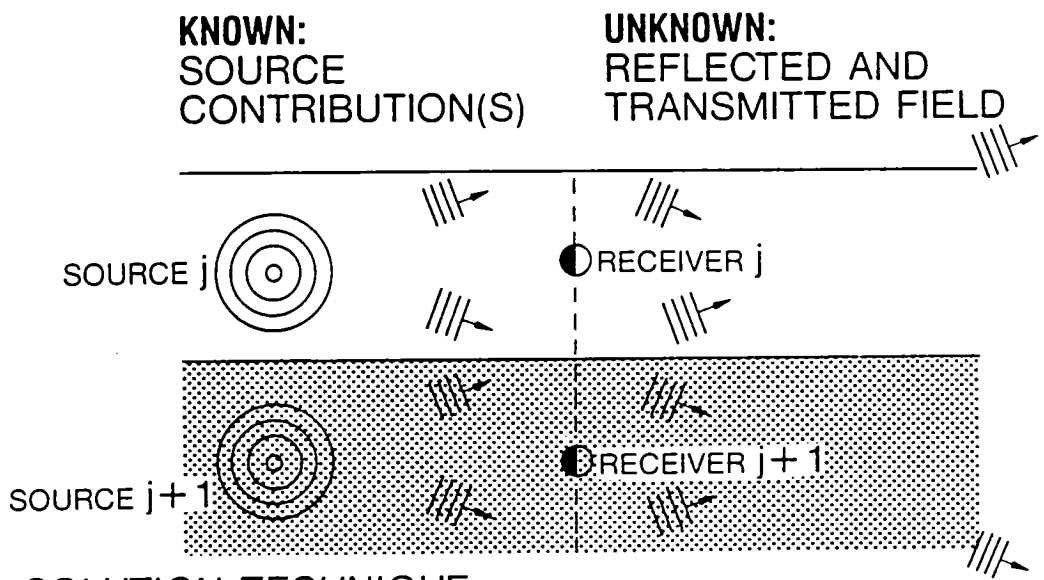

SOLUTION TECHNIQUE

1) SOURCE CONTRIBUTION DECOMPOSED INTO UP AND DOWNGOING PLANE WAVES IN EACH LOCAL LAYER

2) CORRESPONDING PLANE-WAVE COMPONENTS OF UNKNOWN FIELD FOUND BY MATCHING BOUNDARY CONDITIONS IN ALL LAYERS ACROSS ALL INTERFACES

3) TOTAL GLOBAL FIELD AT ALL DEPTHS IS CALCULATED VIA SUPERPOSITION OF ALL LOCAL LAYER WAVEFIELDS
(*DEFINING DEPTH-DEPENDENT GREEN'S FUNCTION*)

4) TOTAL FIELD AT ALL RANGES IS CALCULATED BY NUMERICAL INTEGRATION OF DEPTH DEPENDENT GREEN'S FUNCTION OVER HORIZONTAL WAVENUMBER K_r
(*DEFIING FREQUENCY-DOMAIN TRANSFER FUNCTION*)

5) SYNTHETIC TIME SERIES FOUND BY NUMERICAL INTEGRATION OVER EACH FREQUENCY ω VIA INVERSE FOURIER TRANSFORM
(*DEFINING SYNTHETIC SEISMIC TIME SERIES*)

Figure 1.

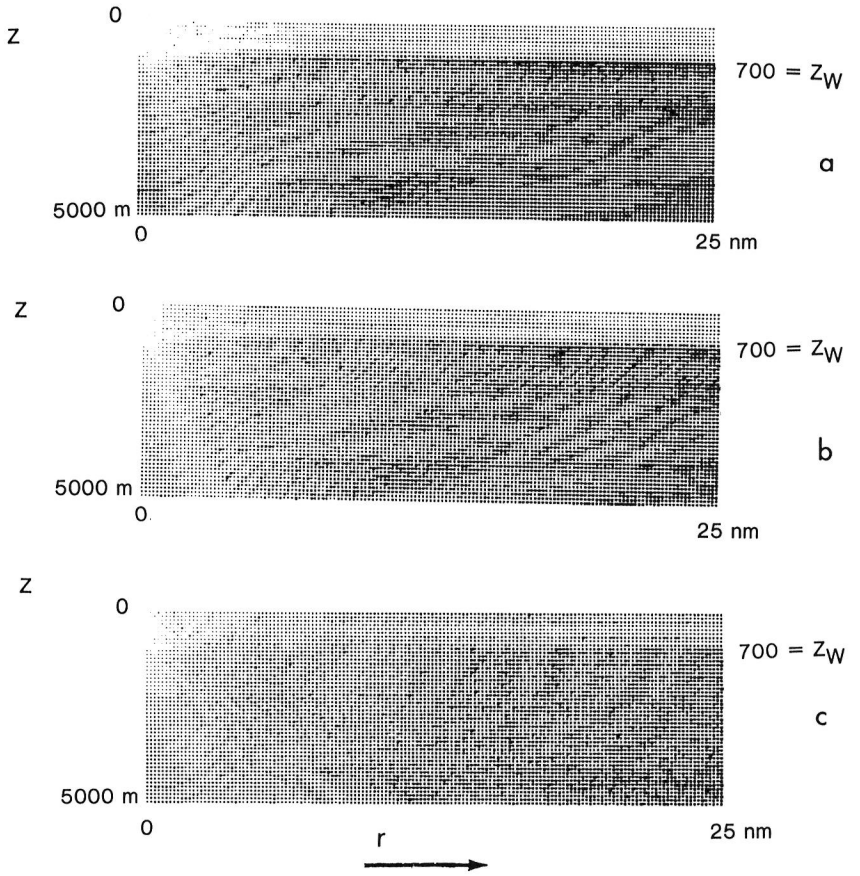

Figure 2. Depth-range contoured transmission loss fields (f = 10 Hz), for horizontal particle velocity (a), vertical particle velocity (b), and normal stress (pressure) (c). Range = 0—25 km; depth = 0—5000 m.

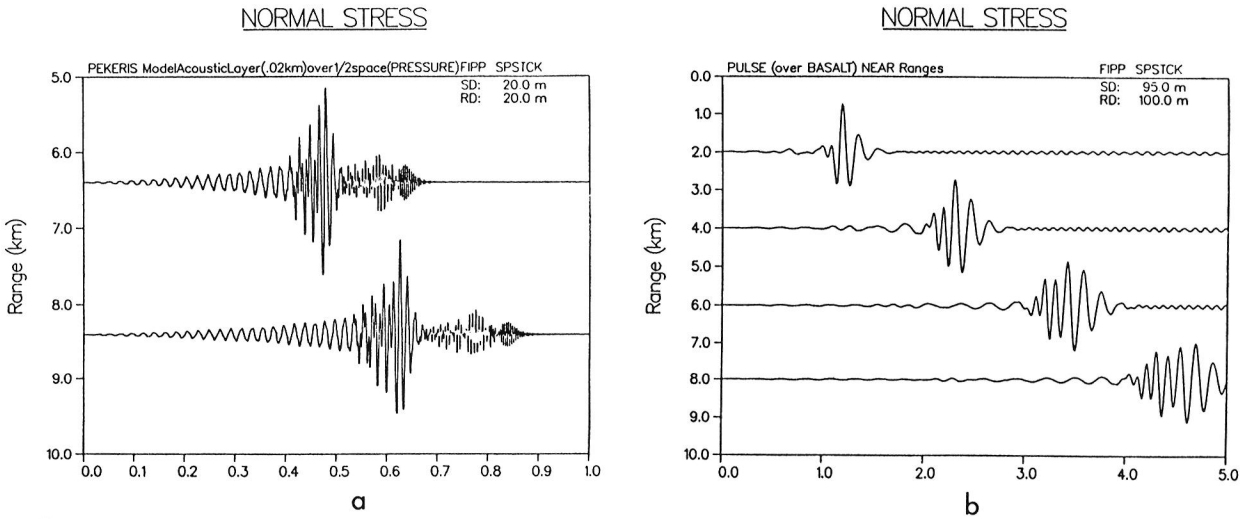

Figure 3. Multifrequency seismic pulse calculations: (a) High-frequency normal acoustic mode (f = 0, 450 Hz; after Pekeris, 1948) at 2 offset ranges, showing direct water and subsequent mode arrivals. (b) Very-low-frequency seismic interface (Scholte) wave (f = 0, 12 Hz) for shallow water waveguide over basalt, showing strong frequency dispersion over 4 offset ranges between 2 and 8 km ranges (after Schmidt, 1982).

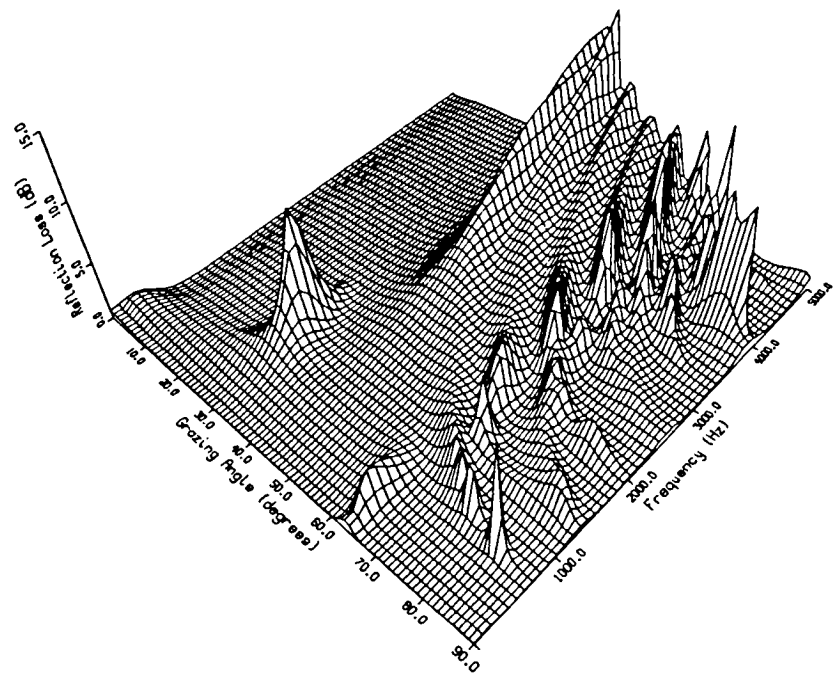

Figure 4a. High-frequency reflection loss as a function of frequency and grazing angle for Arctic under-ice propagation. 2 m thick ice sheet (25 solid layers) overlying 4000 m deep sound channel.

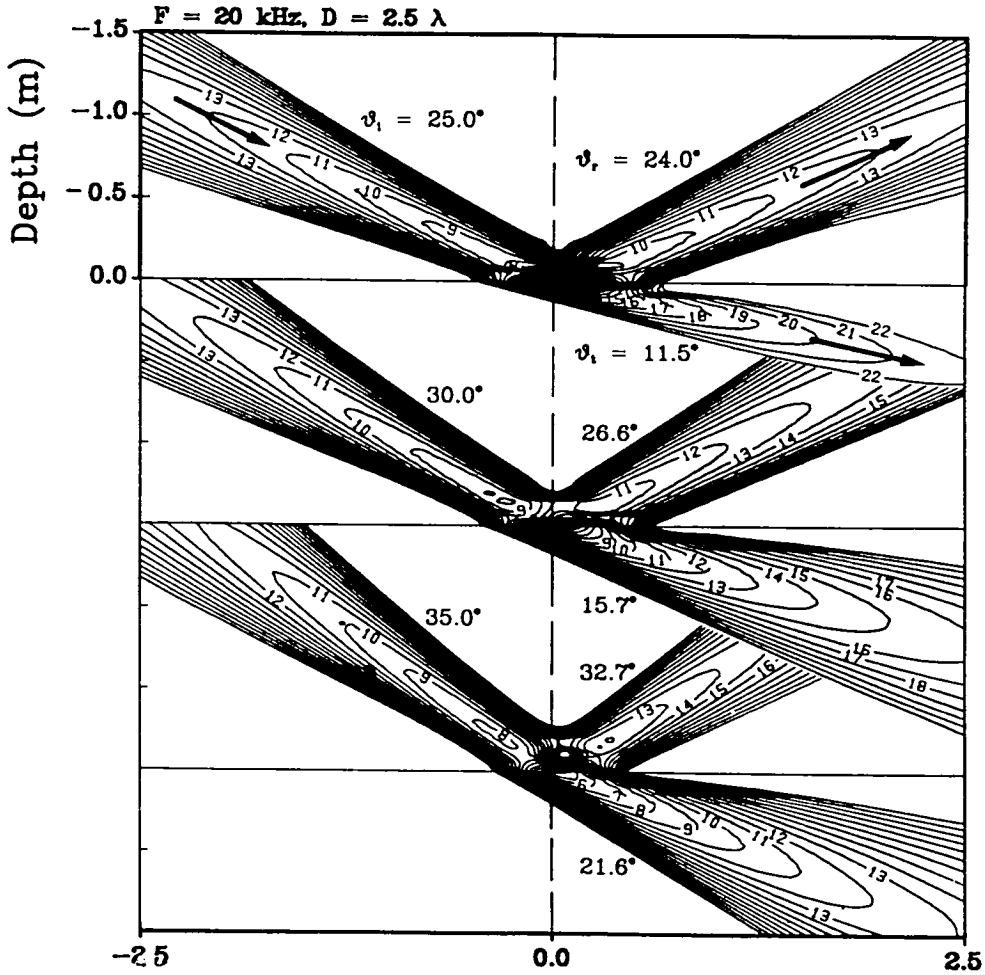

Figure 4b. Very-high-frequency beam reflection and transmission at a water/sand-silt bottom interface (from Schmidt and Jensen, 1984).

NUMERICAL TECHNIQUES FOR SCATTERING FROM SUBMERGED OBJECTS

Michael F. Werby and Gerald J. Tango
National Space Technology Laboratories
NSTL Station, Mississippi 39529-5004

G.C. Gaunaurd
Naval Surface Weapons Center
Silver Spring, Maryland 20910

Scattering from submerged objects consisting of separable boundaries, such as spheres and infinite cylinders, is amenable to closed-form solution by normal mode theory. Results from extensive investigations of these objects has been extremely fruitful in understanding resonance phenomena, background contributions in the absence of resonances, and geometrical effects that give rise to diffraction phenomena. However, when one wishes to examine arbitrary shapes, it is necessary to resort either to approximate theories (valid under limiting assumptions) or numerical methods that adequately treat the problem in question. It has, in fact, proven very difficult to describe scattering from general objects without resorting to frequency-limiting approximations. In this Forum, we describe a numerical procedure, namely, the "extended boundary condition" (EBC) method, together with its applications for treating a variety of problems. The method was established by Waterman[1] for electromagnetic scattering in 1965, and was extended to acoustical scattering by him in 1969[2]. It is sometimes referred to as the "null-field" method in electromagnetism, the "field equivalent principle," or more generally as the T-matrix method. This last nomenclature is unfortunate, since any of a variety of methods can lead to a transition matrix relating the scattered to the incident field, while the EBC or null-field terminology more properly reflects the fact that one is employing a boundary integral technique.

Some of the salutary features of this approach are that (1) the method yields unique solutions to the exterior problem; (2) the transition matrix is independent of the incident field; (3) the method is not frequency-limiting, though it is more efficient for intermediate frequencies; (4) the method can work for a large variety of shapes.

To represent the final results in terms of matrices, one expands all appropriate physical quantities in terms of partial wave basis states. This includes expansions for the incident and scattered fields and the surface quantities (i.e., surface displacement, surface traction, etc.). The method then utilizes the Huygen-Poincaré integral representation for both the exterior and interior solutions, leading to the required matrix equations. One thus deals with matrix equations, the complexity of which depends on the nature of the problem. We show, however, that in general a transition matrix T can be obtained relating the incident field A with the scattered field f having the form $T = PQ^{-1}$, where $f = TA$. The structure of Q can be quite complicated and can itself be composed of other matrix inversions such as arise from layered objects. We focus on recent improvements in this method appropriate for a variety of physical problems, and on their implementation. We outline results from scattering simulations for very elongated submerged objects and resonance scattering from elastic solids and shells. Significant structural improvements such as the coupled higher-order method[3], and the unitary method[4], which lead to more tractable forms of the transition matrix enabling one to avoid matrix inversions and other numerical problems. The final improvement concerns eigenfunction expansions of surface terms, arising from solution of the interior problem, obtained via a preconditioning technique. This effectively reduces the problem to that of obtaining eigenvalues of a Hermitian operator.

This formalism is reviewed for scattering from targets that are rigid, sound-soft, acoustic, elastic solids, elastic shells, and elastic layered objects. We present two sets of the more interesting results. The first concerns scattering from elongated objects, and the second to thin elastic spheroids.

Figure 1 illustrates scattering from a spheroid with aspect ratio 30 for a KL/2 value of 30. Here K is the incident wavenumber and L the object length. We show the case of scattering along the axis of symmetry and 30° and 60° relative to the axis of symmetry and broadside. Elongation effects at 30° and 60° are particularly noticeable where the reflected wave occurs at the same angle as the incident wave relative to the symmetry axis, similar to the plane scattering case. At 0° and 90° the flux is allowed to proceed mainly in the forward direction, with broadside scattering creating the greatest disturbance.

Figure 2a shows resonance phenomena from backscattering from a very thin aluminum spheroid, plotted against KL/2. Scattering here occurs along the axis of symmetry for a spheroid of aspect ratio 3-to-1. Because of the thin nature of the object, its scattering response is like that of a sound-soft object in the absence of resonance. This is verified by subtracting the sound-soft background from the exact elastic calculation, leaving only the resonance response (Figure 2b). Figure 2c is a plot of relative phase for the elastic and sound-soft calculations. Note that the phase is almost zero except at a resonance, where it undergoes a rapid phase-change of 180°, typical of this type of resonance.

REFERENCES

1. P. C. Waterman, "Matrix formulation of electromagnetic scattering," *Proc. IEEE*, 53, 805 (1965).
2. P. C. Waterman, "New foundations of acoustic scattering," *J. Acoust. Soc. Am.*, 45, 1417 (1969).
3. M. F. Werby, "A coupled high-order T-matrix," *J. Acoust. Soc. Am.* (to appear) (1985).
4. M. F. Werby and L. H. Green, "An extended unitary approach-acoustical scattering from elastic shells immersed in a fluid," *J. Acoust. Soc. Am.*, 74, 625 (1983).

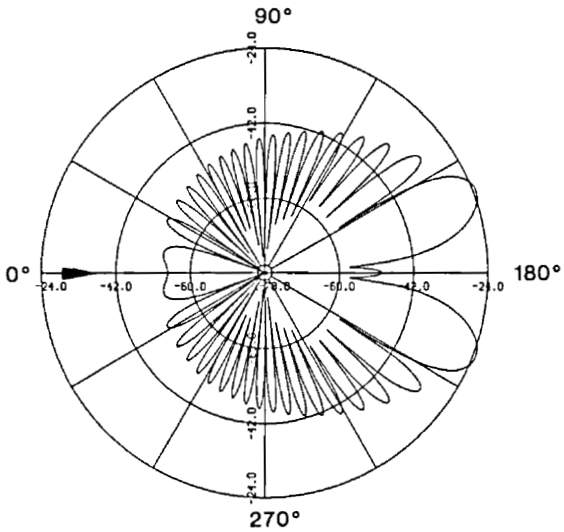

Figure 1a. Scattering along axis of symmetry of spheroid.

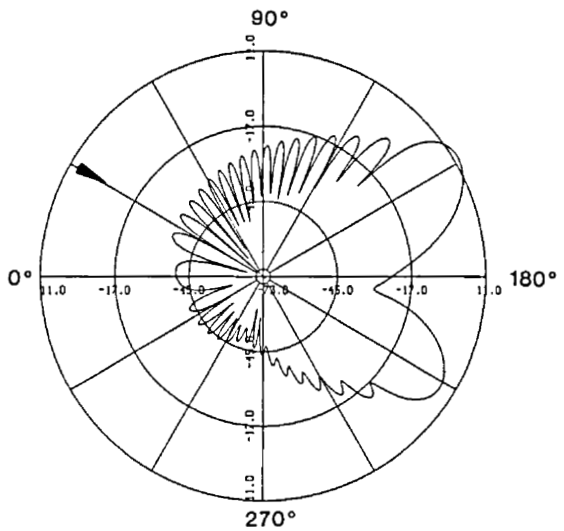

Figure 1b. Scattering at 30° relative to the axis of symmetry of spheroid.

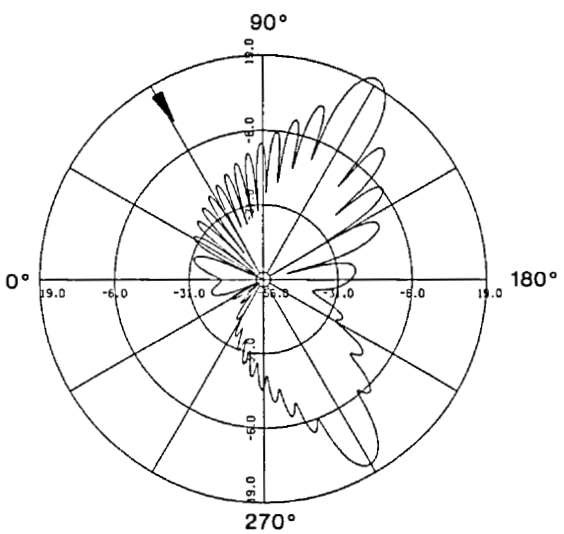

Figure 1c. Scattering at 60° relative to the axis of symmetry of spheroid.

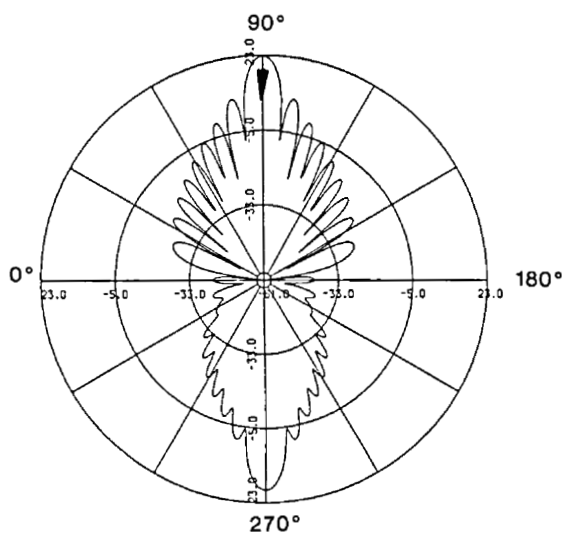

Figure 1d. Broadside scattering from a spheroid.

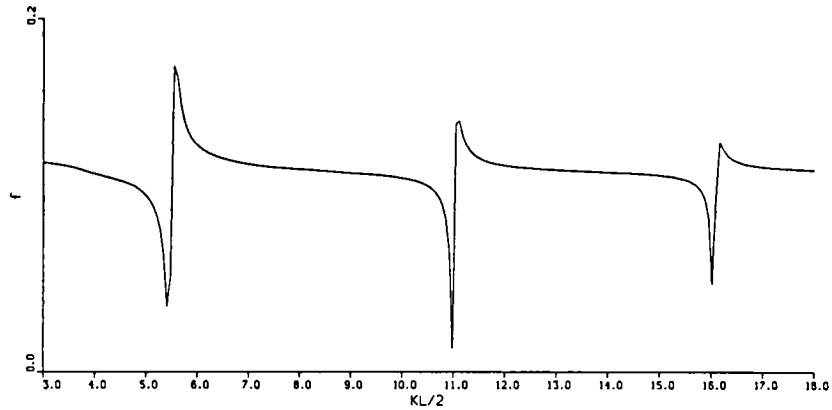

Figure 2a. Form function plot of elastic spheroid end-on incidence.

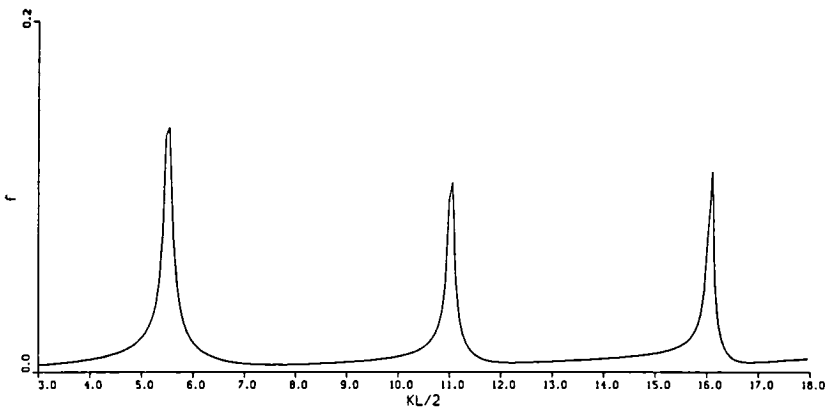

Figure 2b. Resonance response of elastic spheroid end-on incidence.

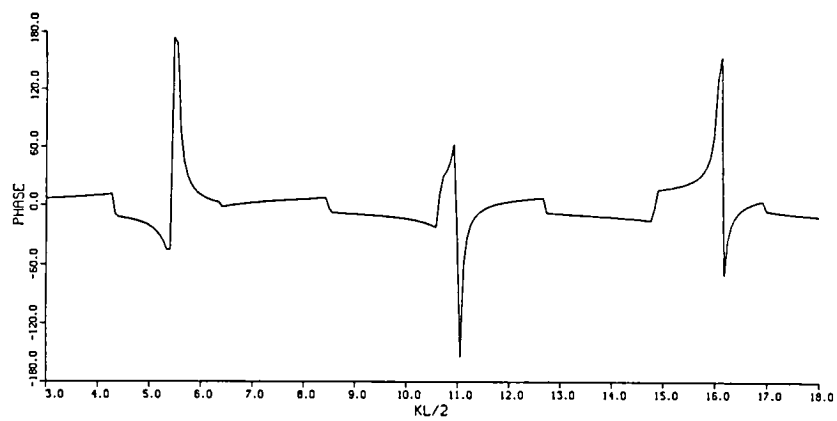

Figure 2c. Relative phase between elastic thin shell and sound-soft object.

PREDICTION OF ACOUSTICAL RESPONSE OF THREE-DIMENSIONAL CAVITIES USING AN INDIRECT BOUNDARY ELEMENT METHOD

Robert J. Bernhard
Purdue University
West Lafayette, Indiana 47907

Carl R. Kipp
Bell Laboratories
Whippany, New Jersey 07981

Boundary Element Methods are numerical techniques used to implement boundary integral equations. In the past, most acoustical boundary element implementations have utilized the Helmholtz Integral Equation or Rayleigh Integral Equation. Such implementations are classified as Direct Boundary Element Methods (DBEM) since the primary variables of the problem, pressure and velocity, are directly solved. Alternatively, as Chen and Schweikert showed [1], the Huygens principle can be cast in the form of a boundary integral equation whereby the unknown variable to be solved is a ficticious boundary source distribution. Such boundary element methods are classified as Indirect Boundary Element Methods (IBEM).

It is the objective of this work to develop a technique which would characterize the acoustics of generalized cavities with the minimum model possible. Potential applications include noise source identification, influence coefficient characterization and active noise control. All boundary element methods have two advantages over finite element methods: 1) the models are smaller, and 2) the assumed variable behavior, inherent in the method to allow discretization, is harmonic rather than polynomial. Further, IBEM often requires one rather than two numerical boundary integrals as required by DBEM. Thus, a quadratic, isoparametric IBEM program was developed for this investigation. It should be pointed out that the source distribution in this solution is continuous and quadratically variable rather than continuous and constant as in Chen and Schweikert's work. The program was also formulated to include the additional capability of interior point sources and impedance boundary conditions.

To test the quadratic, isoparametric IBEM program, several simple cavity enclosure problems where studied. Results are shown in Figs. 1-3. As an aside, the program is easily converted to radiation problems. Several radiation problems were run and the results compare very favorably to numerical solutions to the Helmholtz Integral Equation found in the literature.

The IBEM methods for prediction of acoustical behavior in cavities was found to work quite well. The advantages of IBEM over DBEM or FEM are problem dependent and hence the user should be fully versed in the merits of each. However, we found that for cavity characterization where few pressures are required, IBEM seems most appropriate.

The experience with isoparametric elements suggests one other conclusion. Curved elements introduce substantial complication to the numerical evaluation of the boundary integrals. Thus, wherever appropriate, subparametric elements (i.e. elements with linear geometric interpolation and higher order variable interpolation) are recommended.

[1] L.H. Chen and D.G. Schweikert, "Sound Radiation from an Arbitrary Body," J. Acoust. Soc. Am. 35, 1626-32 (1963).

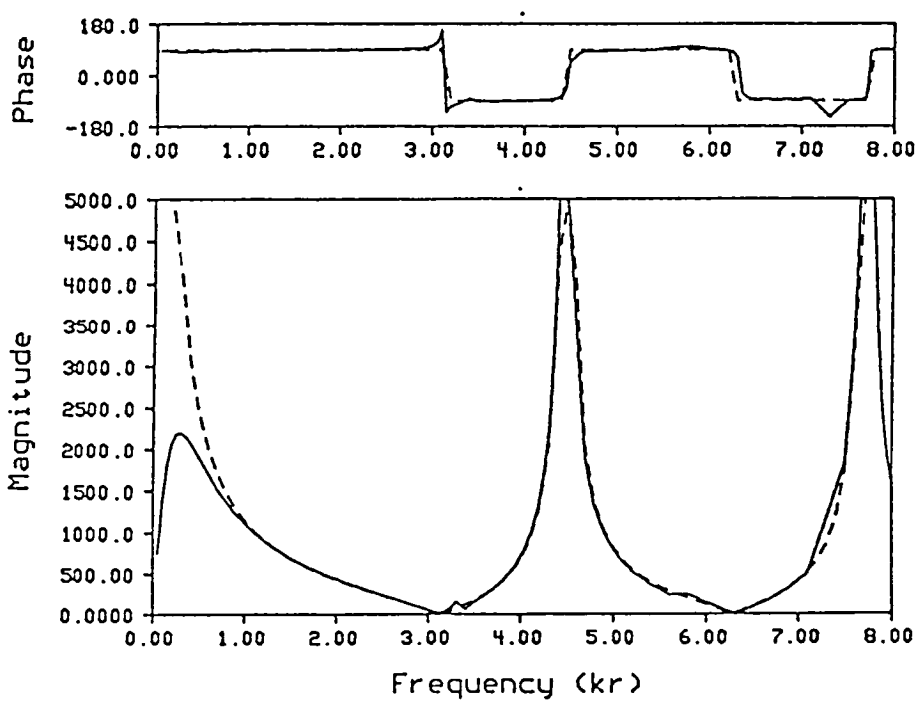

Figure 1. Spherical cavity response - pulsating sphere (r_o = .5); (---) theoretical; (———) predicted

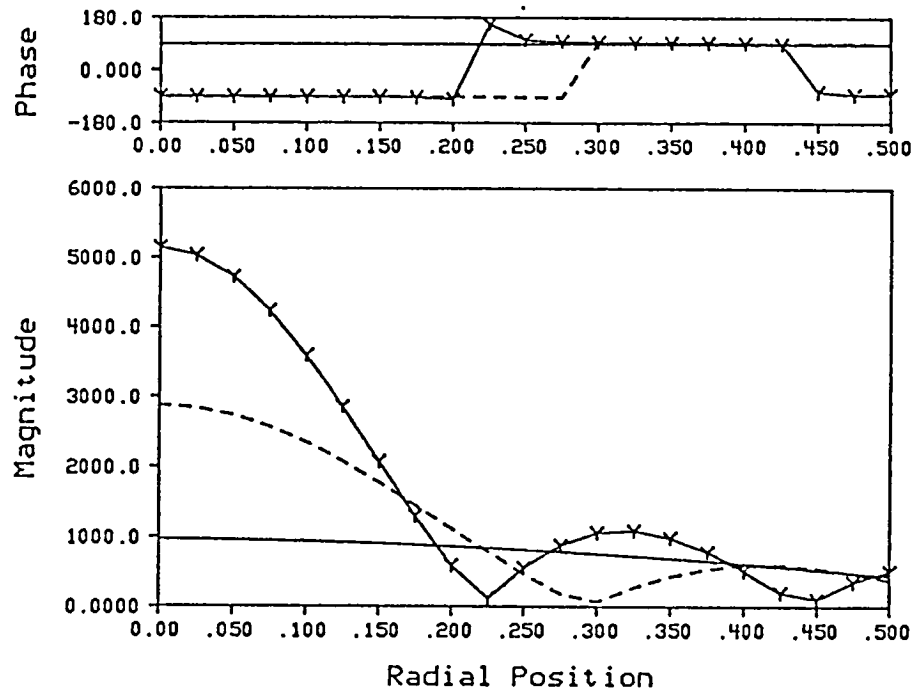

Figure 2. Pressure distribution in pulsating spherical cavity; (———) K = 4.0, (---) K = 10.8, (Y—Y—) K = 14.2.

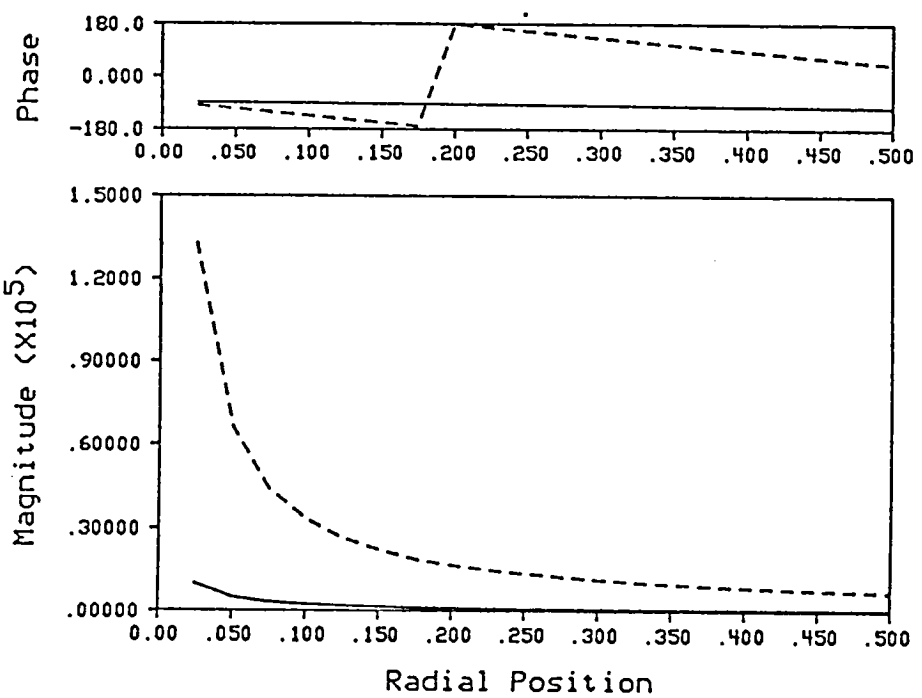

Figure 3. Response of spherical cavity with source at center and radiation boundary conditions; (———) K = .583, (---) K = 8.0.

VORTEX STUDIES RELATING TO BOUNDARY LAYER TURBULENCE AND NOISE

J.L. Adelman
George Washington University
Hampton, Virginia 23665

J.C. Hardin
National Aeronautics and Space Administration
Langley Research Center
Hampton, Virginia 23665

Knowledge of vortex dynamics is crucial to the understanding of boundary layer flow and its noise production, as well as structural fatigue caused by interactions between turbulent flows and various surfaces. The growing use of high-performance aircraft, rotorcraft, and other high-speed transportation systems in recent years has emphasized the need to understand such dynamics, since laminar flow control, interior noise reduction, and structural fatigue characteristics may be critical to the success of such vehicles.

Turbulent boundary layers are comprised of vorticity whose characteristics are defined by the flow direction and surface geometry. As a simple model of a boundary layer, the present study considers the two-dimensional case of an array of N rectilinear, like-sign vortices above an infinite flat boundary. The method of images can be employed with this configuration to reduce the problem to that of 2N vortices in free space, constrained by 2N symmetry relations. This system is Hamiltonian and therefore certain invariants of the motion are known. Further, from the Hamiltonian constant, the equations of motion are readily derived and may be integrated numerically to determine the vortex trajectories. This knowledge of the time-dependent vortex motion then allows the resulting noise radiation to be computed by standard aeroacoustic techniques.

The model has been examined extensively for many different initial vortex configurations, including both trajectory and noise calculations. Several analytical and numerical characteristics of the interactions are observed. For example, for N=2, a criterion,

$$Y_1^{\gamma} Y_2^{1/\gamma}(X^2 + Y_o^2) > \bar{Y}^{\gamma+1/\gamma}(X^2 + Y^2),$$

where Y_1 and Y_2 are the initial heights of the two vortices above the plane, X and Y are their initial separations in the respective coordinate directions, Y_o is twice the average height of the vortices above the boundary, γ is the ratio of the circulations, and $\bar{Y}$ is the centroid of vorticity, for oscillating motion of the vortices can be derived. Such motion is periodic and therefore produces sound spectra containing only harmonically related discrete frequency components. Figure 1a is an example of the vortex trajectories in this case while Figure 1b is the resulting noise radiation to a fixed observer. The apparent modulation of the noise signal is due to the directivity of the noise source as it moves with respect to the fixed observer. When this criterion is not satisfied, the vortex motion is non-oscillating in nature and therefore produces very little noise. Figure 2a is an example of the trajectories in this type of motion while Figure 2b displays the resulting noise. In this case, the influence of the image of the vortex closest to the boundary causes it to convect rapidly away from the other vortex resulting in negligible interaction. The differences between these two cases are similar to those between laminar and turbulent boundary layers.

The analysis is extended for N>2. In this case, the phenomena of non-integrability and non-deterministic "chaotic" solutions occur. Examples of this type of motion are included.

The results of the study indicate that the separation of vortices is an important factor in the noise production of boundary layer flow. Thus, the possibility of control of this separation has implications to the development of turbulence within the boundary layer and its noise radiation and may offer a potential for drag reduction. However, it may prove difficult to obtain even a small degree of control over vortex spacing within a boundary layer. The possibility of doing this must be the subject of future experimental and analytical work.

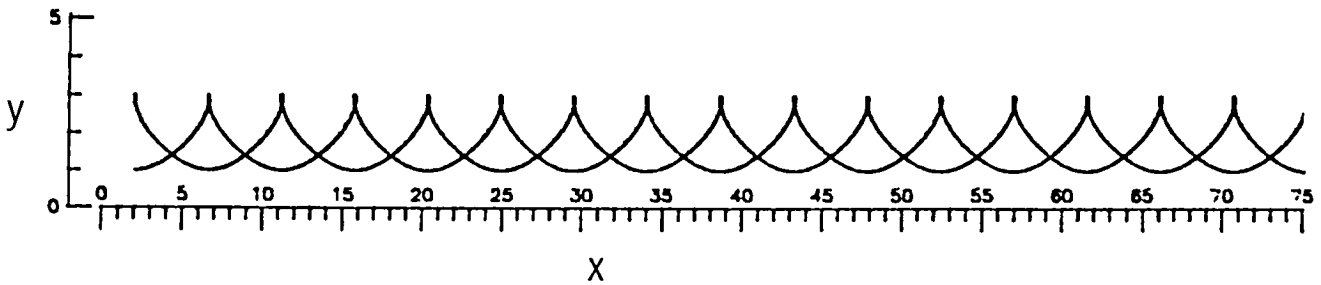

Figure 1a: Vortex Trajectories in Oscillating Case

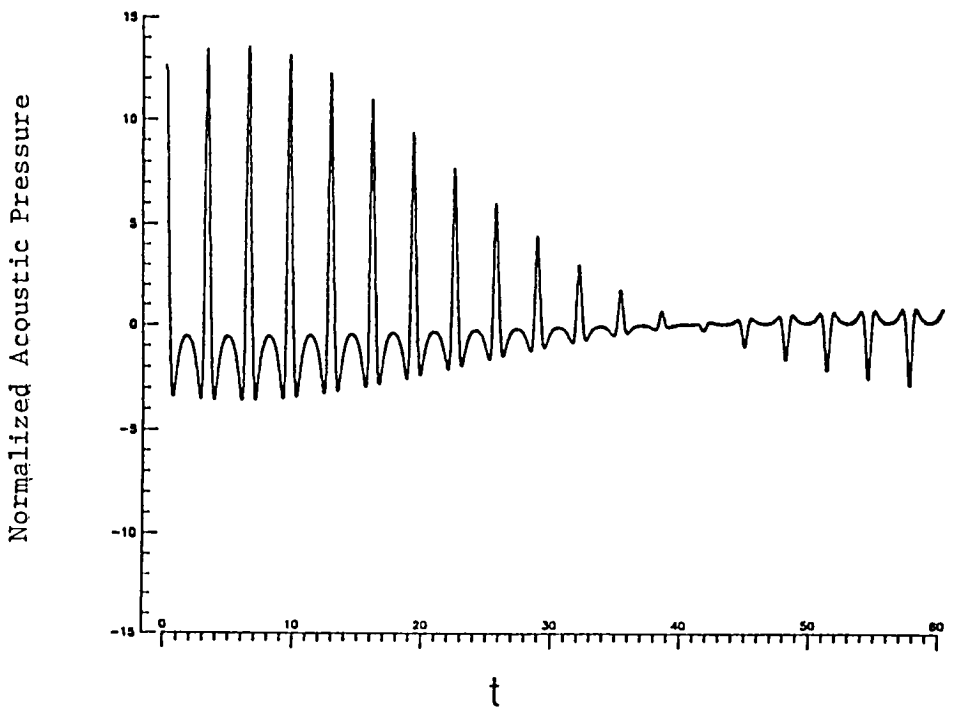

Figure 1b: Acoustic Time History in Oscillating Case

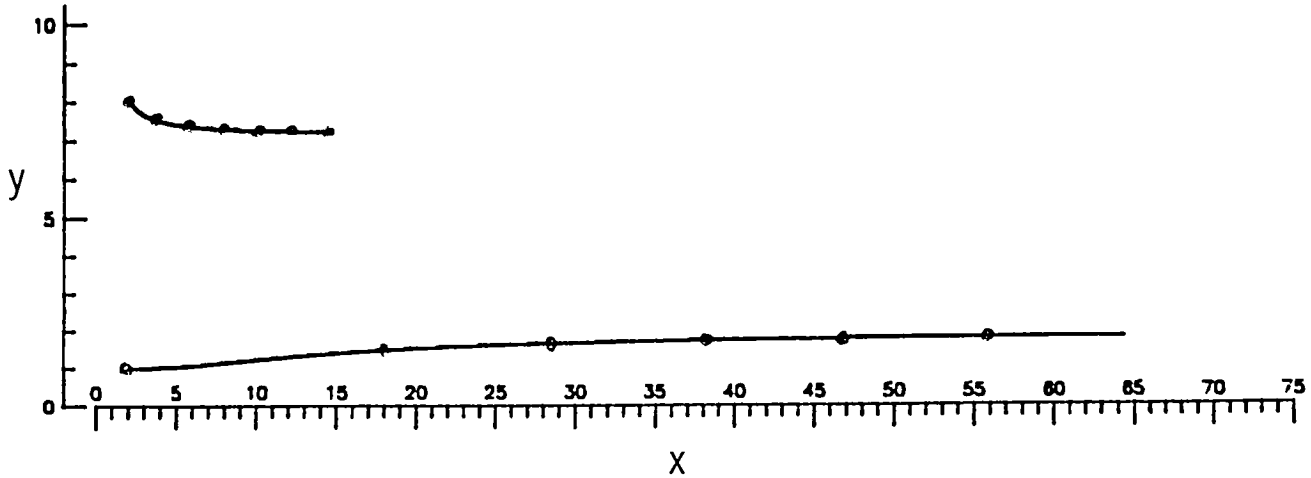

Figure 2a: Vortex Trajectories in Nonoscillating Case

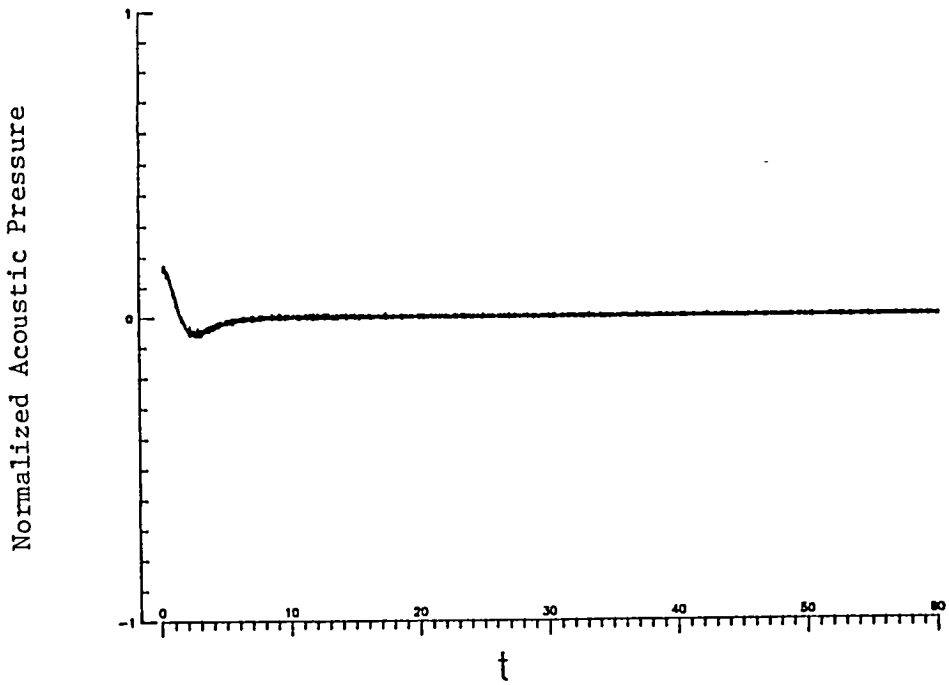

Figure 2b: Acoustic Time History in Nonoscillating Case

STATISTICAL SIGNAL ANALYSIS FOR SYSTEMS WITH INTERFERENCED INPUTS

Robin M. Bai and Anna L. Mielnicka-Pate
Iowa State University
Ames, Iowa 50011

Statistical signal analysis approaches have been successfully used in analyzing acoustical problems which can be modeled as multiple input-one output systems. These methods require well identified and measurable input signals. However, in many physical systems it is not possible to separate all input signals because of the measurement technique used or because of the superposition of several signals at the point of measurement. Conventional and conditioned statistical signal analysis produce significantly distorted results due to input signal interference. This has been described in the literature by a number of investigators as well as discussed in detail by Bendat and Piersol in [1].

The objective of this presentation is to introduce a new approach, based on statistical signal analysis,which overcomes the error due to input signal interference. The model analyzed is shown in Fig. 1. The input signals $u_1(t)$ and $u_2(t)$ are assumed to be unknown. The measurable signals $x_1(t)$ and $x_2(t)$ are interferenced according to the frequency response functions, $H_{12}(f)$ and $H_{21}(f)$.

The goal of the analysis was to evaluate the power output due to each input, $u_1(t)$ and $u_2(t)$, for the case where both are applied at the same time. In addition, all frequency response functions $H_{12}(f)$, $H_{21}(f)$, $H_1(f)$ and $H_2(f)$ are calculated.

The interferenced system is described by a set of five equations with six unknown functions being $u_1(f)$, $u_2(f)$, $H_1(f)$, $H_2(f)$, $H_{12}(f)$ and $H_{21}(f)$. In order to increase the number of equations, three sets of measurements are performed. Each time spectral estimates $S_{x_1x_1}$, $S_{x_2x_2}$, $S_{x_1x_2}$, S_{x_1y} and S_{x_2y} are measured using a Bruel & Kjaer model 2032 Frequency Analyzer (FFT). However, each set of measurements is performed for a different input level. An IBM XT Personal Computer, which was interfaced with the FFT, was used to solve the set of equations.

The software was tested on an electrical two-input, one-output system. The results were excellent. The research presented in this paper includes the analysis of the acoustic radiation from a rectangular plate with two force inputs and the sound pressure as an output signal. The acceleration-pressure frequency response functions calculated on the basis of the conditioned spectral analysis is shown in Fig. 2, from our new approach in Fig. 3, and the one-input, one-output technique (when the second input is physically disconnected) in Fig. 4. The results demonstrate the superiority of the new approach when compared to the conditioned spectral analysis technique. More examples involving the sources absolute and relative contributions in the plate acoustic radiation will be presented and discussed.

[1] Bendat, J. S. and A. G. Piersol, "Engineering Applications of Correlation and Spectral Analysis," J. Wiley & Sons, Chapter 9.3.

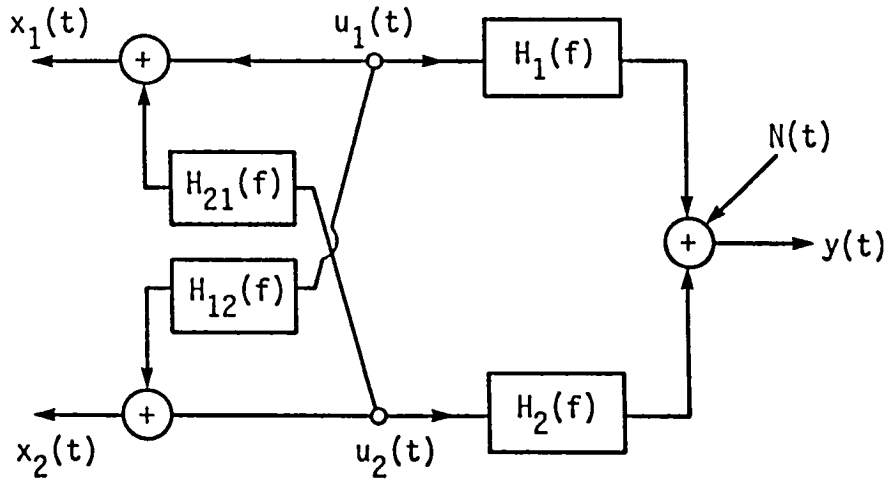

Fig. 1. Interferenced two-input, one-output model

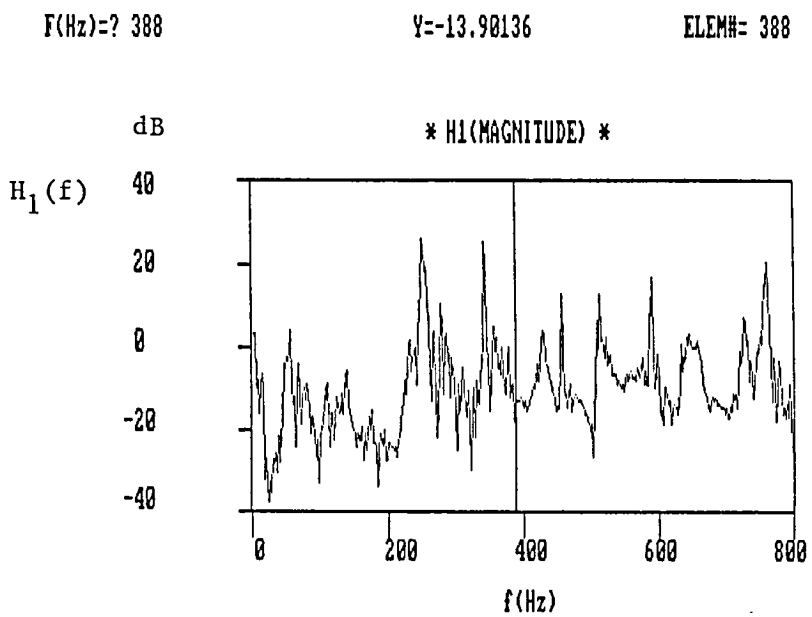

Fig. 2. The frequency response $H_1(f)$ measured using conditioned spectral analysis.

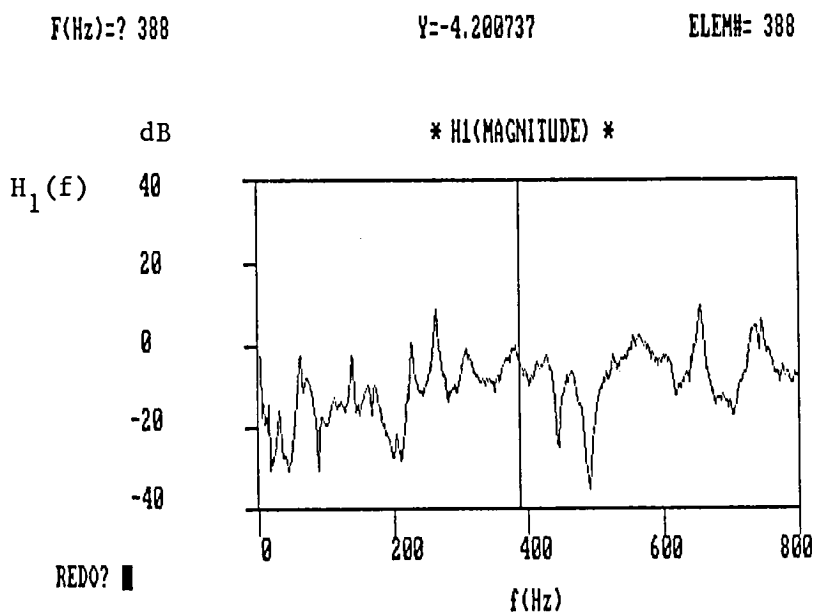

Fig. 3. The frequency response $H_1(f)$ measured using the new approach.

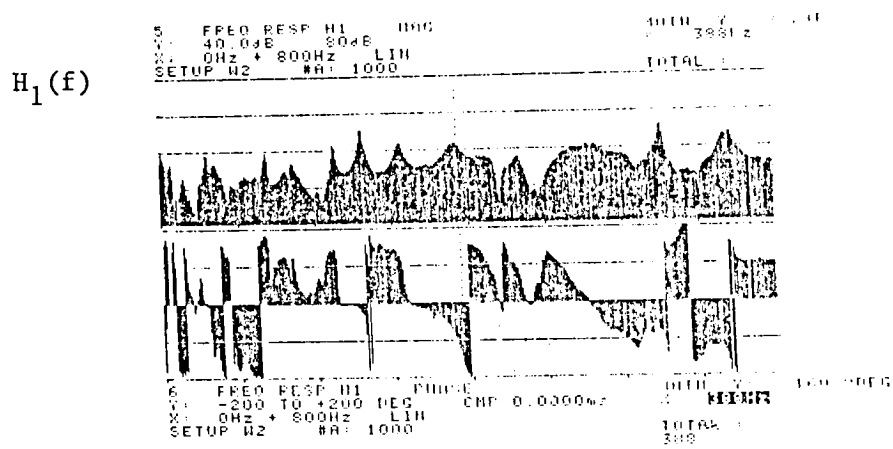

Fig. 4. The frequency response $H_1(f)$ measured using one-input, one-output model.

SOME SEEMINGLY UNRESOLVED QUESTIONS IN NUMERICAL TECHNIQUES IN ACOUSTICS

A. Akay and M. Latcha
Wayne State University
Detroit, Michigan 48202

This is an invitation to the participants and the audience to discuss some questions of continuing interest in the use of Helmholtz Integral and the numerical techniques associated with it.

- Techniques for determing the location and number of interior points to overdetermine the system of equations that results from the surface Helmholtz integral for a general geometry.
- Criteria for the modeling of surfaces in boundary integral method.
- Techniques of solving overdetermined sets of linear equations.
- Other questions on this topic are welcome.

1. Report No.	2. Government Accession No.	3. Recipient's Catalog No.
NASA CP-2404		

4. Title and Subtitle	5. Report Date
Numerical Techniques in Acoustics	October 1985
	6. Performing Organization Code: 505-40-90

7. Author(s)	8. Performing Organization Report No.
Kenneth J. Baumeister, Compiler	E-2758
	10. Work Unit No.

9. Performing Organization Name and Address	11. Contract or Grant No.
National Aeronautics and Space Administration Lewis Research Center Cleveland, Ohio 44135	
	13. Type of Report and Period Covered: Conference Publication
12. Sponsoring Agency Name and Address	14. Sponsoring Agency Code
National Aeronautics and Space Administration Washington, D.C. 20546	

15. Supplementary Notes

16. Abstract

This is the compilation of abstracts of the Numerical Techniques in Acoustics Forum held at the ASME's Winter Annual Meeting in Miami Beach, Florida, November 17-21, 1985. This forum was for informal presentation and information exchange of ongoing acoustic work in finite elements, finite difference, boundary elements and other numerical approaches. As part of this forum, it was intended to allow the participants time to raise questions on unresolved problems and to generate discussions on possible approaches and methods of solution.

17. Key Words (Suggested by Author(s))	18. Distribution Statement
Noise Finite elements Boundary integral	Unclassified - unlimited STAR Category 71

19. Security Classif. (of this report)	20. Security Classif. (of this page)	21. No. of pages	22. Price*
Unclassified	Unclassified		

*For sale by the National Technical Information Service, Springfield, Virginia 22161